Vaccine Discovery and Development: Lessons from COVID-19

Free eBook

Emerging infectious diseases (EIDs) can evolve into a global healthcare crisis or pandemic. Scientists have previously required years to develop vaccines or therapeutics. The use of high throughput technology can greatly broaden the insights collected during discovery, augment efficiency and safety of handling EIDs, and shorten timelines.

Download this publication for an overview of many lessons learned in virology, immunology, and vaccine research during COVID-19 vaccine development.

Download here

SARTORIUS

CURRENT PROTOCOLS
A Wiley Brand

RESEARCH ARTICLE

Conserved C-terminal motifs in odorant receptors instruct their cell surface expression and cAMP signaling

Matthias Kotthoff[1] | Julia Bauer[2] | Franziska Haag[2] | Dietmar Krautwurst[2]

[1]Hamm-Lippstadt University of Applied Sciences, Hamm, Germany

[2]Leibniz-Institute for Food Systems Biology at the Technical University of Munich, Freising, Germany

Correspondence
Dietmar Krautwurst, Leibniz-Institute for Food Systems Biology at the Technical University of Munich, Lise-Meitner-Str. 34, 85354 Freising, Germany.
Email: d.krautwurst.leibniz-lsb@tum.de

Abstract

The highly individual plasma membrane expression and cAMP signaling of odorant receptors have hampered their ligand assignment and functional characterization in test cell systems. Chaperones have been identified to support the cell surface expression of only a portion of odorant receptors, with mechanisms remaining unclear. The presence of amino acid motifs that might be responsible for odorant receptors' individual intracellular retention or cell surface expression, and thus, for cAMP signaling, is under debate: so far, no such protein motifs have been suggested. Here, we demonstrate the existence of highly conserved C-terminal amino acid motifs, which discriminate at least between class-I and class-II odorant receptors, with their numbers of motifs increasing during evolution, by comparing C-terminal protein sequences from 4808 receptors across eight species. Truncation experiments and mutation analysis of C-terminal motifs, largely overlapping with helix 8, revealed single amino acids and their combinations to have differential impact on the cell surface expression and on stimulus-dependent cAMP signaling of odorant receptors in NxG 108CC15 cells. Our results demonstrate class-specific and individual C-terminal motif equipment of odorant receptors, which instruct their functional expression in a test cell system, and in situ may regulate their individual cell surface expression and intracellular cAMP signaling.

KEYWORDS
GPCR, helix 8, intracellular transport, luciferase assay, phylogenetic trees

1 | INTRODUCTION

Bioassay-based evidence, using recombinant odorant receptors (ORs) expressed in a variety of test cell systems, up to date revealed cognate odorant/receptor pairings for only about 19% of all human odorant receptors.[1–11] The major bottleneck for a large-scale assignment of physiologically relevant agonists to human ORs, and other olfaction-related

---

GPCRs ("de-orphaning" or "deorphanization"),[12,13] and thus, for deciphering human odor coding at the receptor level, so far, was the suboptimal expression of recombinant ORs in test cell systems, with obvious variations in cell surface expression and odorant-dependent cAMP signaling between individual OR types. The pioneering work of McClintock and colleagues revealed that in heterologous test cell systems ORs might be retained in the endoplasmic reticulum (ER).[14–17] Recombinant ORs in test cell systems may be posttranslationally modified and largely targeted for degradation.[18] Further, OR genes are prone to be affected by genetic modifications, such as single nucleotide polymorphisms (SNPs),[19–21] leading to allelic variants coding for OR proteins, which may exhibit severely altered ligand binding, signaling, or transport to the plasma membrane.[1,22–24] Several accessory proteins and chaperones have been identified that are involved in transport of ORs or their G protein alpha subunits to the ciliary plasma membrane of olfactory sensory neurons, or to the cell surface of test cell systems.[25–29]

For many integral membrane proteins, for example, transmembrane proteins, such as G protein-coupled receptors (GPCR) and ion channels, it is well known that their intracellular transport correlates to their equipment with evolutionary conserved, short intracellular amino acid (AA) motifs (Tables 1 and 2). These motifs may act as a transporting handle in protein-protein interactions serving intracellular protein homeostasis mechanisms. For example, the association between a GPCR's C-terminal membrane-proximal AA motif of basic residues and the coatomer protein I complex (COPI) may arrest this receptor within intracellular compartments, whereas its C-terminal interaction with, for example, 14-3-3 proteins may promote its cell surface expression.[30–33]

TABLE 1 C-terminal motifs related to ER localization/retention

Motif	Molecule and motif position	Motif location relative to plasma membrane	Interaction	References
RR	Tmed2$_{163-164}$ (*C. griseus*)	md	COPI	95,96
	TAS1R2$_{837-838}$	md	TAS1R3	97
RxR	Kir6.2$_{369-371}$	md	-	78,98,99
	TMX4$_{338-340}$	md	-	100
	Pmp2p_C-term$_{Kir6.2}$ chimera	md	Bmh1p	101,102
	GPR15$_{352-354}$	md	YWHA	32
	CD8_ C-term$_{GPR15}$ chimera	md	-	77
	LMAN2L$_{344-346}$	md	-	103
	Gabbr1$_{922-924}$ (rat)	md	Gabbr2	34
	GABBR1a$_{923-925}$	md	GABBR2	35
KKxx or KK-COOH	TMED9$_{232-233}$	md	COPI	104,105
	GST_WBP1$_{427-428}$ chimera	md	COPI	106,107
	CD4_, CD8_, HLA-A_ E3/19K$_{156-157}$ chimera	md	-	108–110, but see: 111
	GFP_CF9_GPAT8$_{499-500}$, chimera	md	-	112
KxKxx	CNGA1$_{650-652}$	md	-	113
	CNGA1$_{652-654}$ (bovine)	md		
	CNGA2$_{628-630}$,(bovine)	md		
	SACM1L$_{583-585}$	md	COPI	114
	TMED10$_{213-215}$	md	COPI	104,105
K(D/E)xL	Hspa5$_{583-585}$ (rat)	md	-	62

Abbreviations: Bmh1p, 14-3-3 family protein BMH1 (*S cerevisiae*); CD4, CD4 molecule: coreceptor with the T-cell receptor; CD8, CF9, Carbohydrate-binding protein; CNGA1, rod cyclic nucleotide-gated cation channel; CNGA2, olfactory cyclic nucleotide-gated cation channel; COPI, coatomer protein complex I, coats vesicles transporting proteins from the cis-Golgi complex back to the rough endoplasmic reticulum; E3/19K immune modulating protein (GP19K, human mastadenovirus C), adenoviral type I transmembrane protein; Gabbr1, Gabbr2, rat gamma-aminobutyric acid (GABA) B receptor subunits 1 and 2, GABBR1, GABBR2, human GABA B receptor subunits 1 and 2; GFP, green fluorescent protein; GPAT8, glycerol-3-phosphate acyltransferase 8 (A. thaliana); GPR15, G protein-coupled receptor 15, chemokine GPCR for human immunodeficiency virus type 1 and 2; HLA-A, major histocompatibility complex, class-I, A molecule; Hspa5(GRP78), heat shock protein family A (Hsp70) member 5; Kir6.2, KATP channel; LMAN2L(VIPL), lectin, mannose binding 2 like, type I transmembrane protein; md, membrane-distal; Pmp2, yeast proteolipid ATPase; SACM1L, SAC1-like phosphatidylinositide phosphatase; TAS1R2, sweet taste receptor subunit; Tmed2, transmembrane p24 trafficking protein 2; TMED9(p25, p24d), transmembrane p24 trafficking protein 9; TMED10(p23, p24c), transmembrane p24 trafficking protein 10; TMX4, thioredoxin-related transmembrane protein 4: ER oxidoreductase; WBP1, yeast dolichyl-diphosphooligosaccharide-protein glycoltransferase; YWHA, tyrosine 3-monooxygenase/tryptophan 5-monooxygenase activation proteins, 14-3-3 family protein.

TABLE 2 C-terminal motifs related to ER/Golgi export and/or plasma membrane translocation

Motif	Molecule and motif position	Motif location relative to plasma membrane	Interaction	References
RR	GPR15$_{310-311}$	mp	-	31
	B3galt4$_{7-8}$ (mouse), B4GALNT1$_{5-6}$ N-term. = cytoplasmic tail	mp	Sar1, Sec23p, COPII	88
VxP	RHO$_{345-347}$	md	Arf4	115
	Cngb1$_{1315-1317}$ (rat)	md	-	116
LL	ADRB2$_{339-340}$	mp	Rab8	117,118
	AVPR2$_{339-340}$	mp	-	82,119
	Drd1$_{344-345}$ (rat)	mp	-	30
	Kcnd2$_{481-482}$ (rat)	mp	-	120
	IL2RA_CD3G$_{153-154}$ chimera	mp	-	121
LL and LI	Slc12a1$_{LL1033-1034,\ LI1043-1044}$ (mouse)	mp	-	89
FR	Smo$_{W549-R550}$	mp	-	122
	ODR-10$_{308-309}$, (*C. elegans*)	mp	-	123
FF	TMED9$_{228-229}$, TMED10$_{211-212}$	mp	COPI	105
FxxxFxxxF	Drd1$_{333-341}$ (rat)	mp	Dnajc14	124
	Drd1$_{333-341}$ (rat)	mp	γ-COPI	30
RxR	ST8SIA1$_{6-8,\ 25-27}$, N-term. = cytoplasmic tail	mp	Sar1, Sec23p, COPII	88

Abbreviations: ADRB2, adrenoceptor beta 2; Arf4, ADP ribosylation factor 4; AVPR2, arginine vasopressin receptor 2; B3galt4(GALT2), beta-1,3-galactosyltransferase 4; B4GALNT1(GalNAcT), beta-1,4 N-acetylgalactosaminyltransferase 1 isoform X2; CD3G, CD3-gamma polypeptide; Cngb1, cyclic nucleotide-gated channel subunit beta 1; COPI, coatomer protein complex I; COPII, coatomer protein complex II; COPG1, COPI coat complex subunit gamma 1; Dnajc14(Drip78), DnaJ heat shock protein family (Hsp40) member C14; Drd1, dopamine receptor D1; GPR15, G protein-coupled receptor 15; HSPA5, heat shock protein family A (Hsp70) member 5; IL2RA(Tac), interleukin 2 receptor subunit alpha; Kcnd2 (Kv4.2), potassium voltage-gated channel subfamily D member 2; md, membrane-distal; mp, membrane-proximal; Odr-10, olfactory receptor Odr-10; RHO, rhodopsin; Sar1, COPII coat GTPase; Sec23p, COPII coat component; Slc12a1(Nkcc2), solute carrier family 12, member 1; Smo, smoothened, frizzled class receptor; ST8SIA1(SialT2), ST8 alpha-N-acetylneuraminide alpha-2,8-sialyltransferase isoform 1; TMED9(p25, p24d), transmembrane p24 trafficking protein 9; TMED10(p23, p24c), transmembrane p24 trafficking protein 10.

Another example is the hetero-dimerization of the two subunits GABBR1 and GABBR2 of the GABA$_B$-receptor by which a membrane-distal C-terminal "RxRR" motif is masked or dislocated, which otherwise functions as an ER-retention handle.[34,35] It has been suggested that the receptor transport protein RTP1S may act on the expression of at least a portion of ORs in a similar way.[26,28]

A few studies failed, however, to identify any conserved AA motifs in ORs,[18,36–38] such as "KDEL," "KKxx," or "RxR" sequences that typically are involved in, for instance, ER retention/retrieval or Golgi to ER recycling of integral membrane proteins (Table 1). In sharp contrast, several studies unambiguously pointed out conserved patterns of at least membrane-proximal, basic AAs within the C-termini of ORs,[31,39–41] some of which overlapped with amphiphilic helix 8, a C-terminal structure in many GPCRs that was originally identified in rhodopsin,[42] and later also in ORs.[43,44]

We therefore hypothesized, that ORs, like many GPCRs, are indeed equipped with conserved, C-terminal AA motifs, which may be attributable to the ORs' individual or even class-specific plasma membrane expression and/or cAMP signaling.

Here, we set out to identify highly conserved and class-specific C-terminal AA motifs in ORs, by statistical and phylogenetic in silico analyses of 4808 odorant receptors across eight species from zebrafish to man. We interrogated the impact of some conserved motifs and their AAs on the functional expression of ORs by site-directed mutagenesis, and by measuring odorant-dependent cAMP signaling of recombinant, IL-6/Halo-tagged receptors in NxG 108CC15 cells using the GloSensor assay.[45–47] We further quantified the cell surface expression of all receptor constructs by flow cytometry.

2 | MATERIALS AND METHODS

2.1 | Chemicals

The following chemicals were used: Dulbecco's MEM medium (#F0435), FBS superior (#S0615), L-glutamine (#K0282), penicillin (100 U/ml)/streptomycin (100 U/ml) (#A2212), trypsin/EDTA solution (#L2143) (Biochrom, Berlin, Germany), MEM nonessential amino acid solution

(100x) (#M7145, Sigma-Aldrich, Steinheim, Germany), and Gibco HAT supplement (#21060-017, Thermo Fisher, Dreieich, Germany).

Further were used: CaCl$_2$*2H$_2$O (#22322.295), D-glucose (#101174Y), dimethyl sulfoxide (DMSO) (#83673.230), HEPES (#441476L), potassium chloride (#26764.230), and sodium hydroxide (#28244.295) (VWR Chemicals BDH Prolabo, Leuven, Belgium), sodium chloride (#1064041000, Merck, Darmstadt, Germany), D-luciferin (beetle) monosodium salt (#E464X), and HaloTag Alexa Fluor 488 Ligand (#G1001, Promega, Madison, USA).

(-)-Carvone, sotolone, lyral, and butyric acid were purchased from Sigma-Aldrich (Steinheim, Germany). 3-Mercapto-2-methylpentanol was purchased from Chemos GmbH (Regenstauf, Germany).

2.2 | Cloning and site-directed mutagenesis of OR-coding regions

The receptor constructs were either amplified by polymerase chain reaction (PCR) or PCR-based site-directed mutagenesis using the Phusion hot start DNA-polymerase (#F549S, Thermo Scientific, Waltham, USA) with the primers listed in Tables S1-S14.

The OR-coding regions were ligated with T4 DNA ligase (#M1804) EcoRI/NotI (#R6017/#R6435) into the expression plasmid pFN210A (#pFN210A SS-HaloTag CMV-neo FlexiVector, Promega, Madison, USA).[5,47]

2.3 | Cultivation of Cells

We used NxG 108CC15 cells[46] as a test cell system for the functional expression of recombinant ORs. NxG 108CC15 cells were cultivated as described in.[48]

2.4 | Luminescence Assay

One day pretransfection, NxG-cells were plated in a 96-well format (Thermo Scientific Nunc F96 MicroWell, white, #137103, Thermo Fisher Scientific Inc, Waltham, USA) with a density of 7,500 cells per well. The transfection was performed using Lipofectamine 2000 (#11668019, Thermo Fisher Scientific Inc, Waltham, USA), 100 ng plasmid-DNA and each 50 ng Gαolf, Gγ13, RTP1S, and pGloSensor-22F-cAMP (Promega, Madison, USA[45]) each. As a control the transfection was performed with the vector plasmid pFN210A lacking any OR-coding region, together with Gαolf, Gγ13, RTP1S, and cAMP-luciferase pGloSensor-22F. The amount of transfected plasmid-DNA was equal in OR-transfected and mock-transfected cells.

Luminescence assays were performed 42 h post transfection as reported previously.[48]

The effective stimulus concentration yielding 50% effect (EC$_{50}$) and concentration-responses curves were derived from fitting the function.

$$f(x) = \left(\frac{(min - max)}{\left(1 + \left(\frac{x}{EC_{50}} \right)^{Hillslope} \right)} \right) + max$$

to the data by nonlinear regression (SigmaPlot 10.0, Systat Software). All data are presented as mean $\pm$ SD.

2.5 | Flow cytometry

NxG 108CC15 cells were cultivated in 12-well plates with a density of 80,000 cells per well. On the next day the transfection was performed as described earlier.[48]

For analysis, cells were harvested 42 hours post transfection and stained with the cell-impermeant HaloTag Alexa Fluor 488 Ligand (ex/em = 499/518 nm). Cells were incubated for 1 hour at 37°C and 7% CO$_2$ in the cell culture incubator. Cells were washed twice with serum-free medium prior to FACS analyses (MACSQuant Analyzer, Miltenyi Biotec, Bergisch Gladbach, Germany). A forward- and side-scatter gate was set to exclude dead cells with forward-scatter (FSC: 235V) and side-scatter (SSC: 360V). The FITC signal (B1-channel; HaloTag Alexa Fluor 488 Ligand) was detected with 175V. In each case, 10,000 cells were measured. The analysis was performed with the Macs Quantify analysis software (Miltenyi Biotec B.V. & Co. KG, Bergisch Gladbach, Germany). All receptors were measured at least three times and normalized to the wild-type (wt) receptor maximum signal.

2.6 | Bioinformatics

NCBI and HORDE were used as databases for the retrieval of genetic information on *Homo sapiens* (human), *Mus musculus* (mouse), *Bos taurus* (cow), *Monodelphis domesticus* (opossum), *Ornithorhynchus anatinus* (platypus), *Gallus gallus* (chicken), *Xenopus spec.* (clawed frog), and *Danio rerio* (zebrafish) chemosensory receptor genes.[49,50] After revision (ie, deletion of partial sequences and duplicates) of the final 4808 sequences, the individual sequences were assigned to phylogenetic classes I (807) or II (4001), and processed separately. Total number of ORs analyzed per species are listed in Table S15. For the distribution and mutational analysis of AA motifs in ORs, we used a threshold of ≥5% across an OR repertoire to detect the presence

of motifs, since the probability that two out of 20 AA occur randomly in a certain order is 5%. The ClustalW alignments were fixed to P6.50 assuring proper assignment of receptor domains in all ORs of any species.[51] The phylogenetic reconstruction of ORs was performed with CLCbio[52] and MEGA5 software.[53] Therefore, in a first step, all retrieved GPCR sequences were aligned using ClustalW algorithm.[54] The evolutionary history was inferred using the Neighbor-Joining method[55] followed by 500 bootstrap replications.[56] Scale bar refers to the evolutionary distances, computed using the Poisson correction method[57] and are given in the units of the number of AA substitutions per site. Evolutionary analyses were conducted in MEGA5.[53] For rooting the constructed tree, human rhodopsin (NCBI entry: NP_000530.1) was used as an out-group. All statistical methods were performed with Office Excel (Microsoft), the Excel Add In Multibase 2015 (Numerical Dynamics), SigmaPlot (Systat Software, Inc), R! (r-project.org), and the web tool "WebLogo" [available at http://weblogo.threeplusone.com; Ref. 58].

When testing for differences between two groups, we used the Shapiro-Wilk normality test and the Brown-Forsythe equal variance test as criteria to use the Student's two-tailed t test, or, when applicable and in line with our experimental strategy to test our working hypotheses, the Student's one-tailed t test in SigmaPlot 14 (Systat Software, Inc).

To test for differences between the means of two distributions (number of C-terminal motifs per receptor in class-I vs class-II ORs), we used a left-tailed z-test, with the 0-hypothesis H0: $\bar{x}1$(class-I ORs) = $\bar{x}2$(class-II ORs), the alternative hypothesis Ha: $\bar{x}1$(class-I ORs) $< \bar{x}2$(class-II ORs), a level of significance of $\alpha = 0.05$, and a corresponding critical z-value of -1.645, using the formula: $z = \dfrac{\bar{x}_1 - \bar{x}_2}{\sqrt{\frac{\sigma_1{}^2}{n_1} + \frac{\sigma_2{}^2}{n_2}}}$.

We used the R! packages "ggpubr," "ggscatter," and "ggplot2" to obtain Spearman's correlation with confidence intervals on the number of C-terminal motifs per OR over evolution.
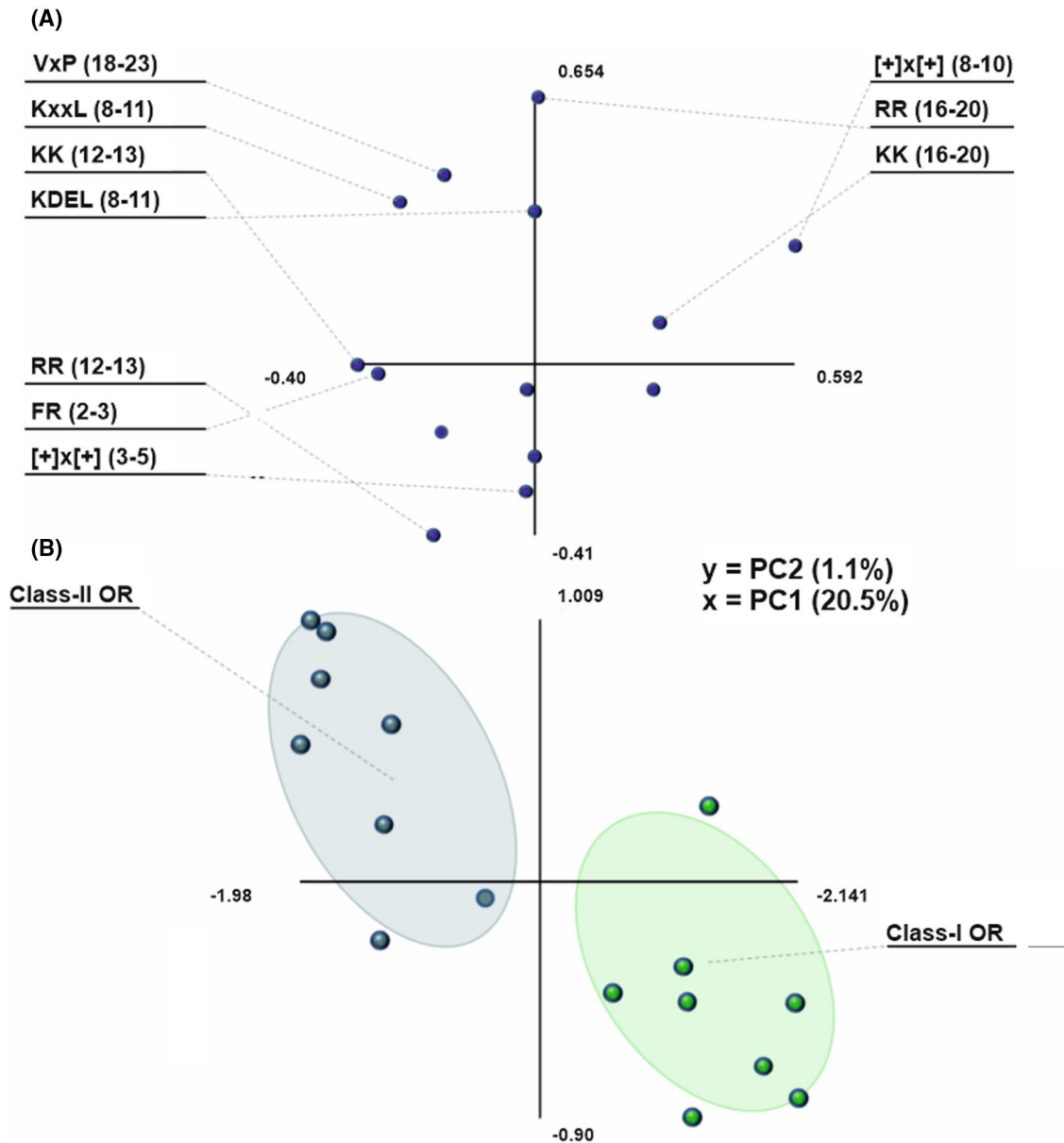
3 | RESULTS

Given the published evidence of functional C-terminal AA motifs in integral membrane proteins (Tables 1 and 2), such as GPCRs, we put 4808 ORs from eight species to the test by investigating (**i**) whether any of the published C-terminal motifs are present in the C-termini of ORs, and (**ii**) whether class-I and class-II ORs separate according to their equipment with distinct motifs.

3.1 | Conserved C-terminal short amino acid motifs in ORs discriminate between class-I and class-II receptors

We observed a sharp and nonoverlapping difference of class-I and class-II ORs, by means of a partial least squares-differential analysis (PLS-DA), with respect to ORs'-specific equipment with motifs from Tables 1 and 2 (Figure 1). Many of these motifs occur solely class-specific, such as the dibasic "[+]x[+]" motif at C-term$_{8-10}$ in class-I ORs, or the dibasic "[+][+]" motif at C-term$_{12-13}$ in class-II ORs (Figure 2A, Table 3). C-terminal numbering starts after Y7.53.[59] Moreover, the specific constitution of these motifs is class-specific, for example, the dominant "[+]x[+]" motif at C-term$_{3-5}$, which occurs at high rates in either class, is predominantly a "KxK" in class-I ORs, but a "RxK" or "RxR" in class-II ORs, and has been shown previously to be highly conserved within ORs.[31,40,41] As the variables plot in Figure 1 shows, the major contributors to the differentiation of class-I and class-II ORs are the class-I-specific "[+]x[+]" motif at C-term$_{8-10}$, and the class-II-specific "[+][+]" motif at C-term$_{12-13}$ (Figure 1A). As expected, a generalized "[+]x[+]" motif at C-term$_{3-5}$ did not add to the differentiation of class-I and class-II ORs. Neither did "FR" at C-term$_{11-18}$, "KxxL" at C-term$_{12-15}$, "LL" at C-term$_{14-15}$, or "FF" at C-term$_{14-18}$.

We thus set out to characterize conserved motifs in OR's C-termini by large-scale in silico analyses of their AA sequences.

Analyzing 4808 aligned AA sequences of the available OR repertoires of eight species from zebrafish to human (Table S15), we found that 86.2% of all class-I ORs (mainly encoded by group α OR genes, except zebrafish comprising groups β, ε-η[60]), and 94.7% of class-II ORs (mainly encoded by group γ OR genes[60]), are equipped in their C-termini with at least one of known motifs related to intracellular transport, as listed in Tables 1 and 2, at abundancies >5% (Figure 2A). Counting all 133 zebrafish ORs as class-I ORs may not be entirely correct. Sixty-eight out of 133 *d. rerio* ORs investigated, however, are equipped with a single out of three C-terminal motifs found at an abundancy >5%, which are mutually exclusive, except for four ORs (drORE1241-43, drOR15), which carry two motifs. Of those 68 ORs, notably, 14 receptors carry the class-I OR-specific single-spaced, dibasic [+]x[+] motif at C-term$_{8-10}$, which is basically absent in class-II ORs (abundance: 0.35%). Thirty-five fish ORs (26.3%) carry a single-spaced, dibasic [+]x[+] motif at C-term$_{13-16}$, three fish ORs (2.3%) carry a single-spaced, dibasic [+]x[+] motif at C-term$_{16-20}$, and 19 fish ORs (14.3%) carry a dibasic [+][+] motif at C term$_{16-20}$ (Figure S1, Supplemental material Mendeley Data, V1, https://doi.org/10.17632/49n4t7b4r2.1). Interestingly, and in contrast to the overall

(A)

VxP (18-23)

KxxL (8-11)

KK (12-13)

KDEL (8-11)

0.654

[+]x[+] (8-10)

RR (16-20)

KK (16-20)

RR (12-13)

FR (2-3)

[+]x[+] (3-5)

-0.40

0.592

-0.41

$y = PC2 (1.1\%)$
$x = PC1 (20.5\%)$

1.009

(B)

Class-II OR

-1.98

-2.141

Class-I OR

-0.90

FIGURE 1 C-terminal amino acid motifs discriminate between class-I and class-II ORs. A, Variables plot of a PLS-DA of C-terminal motifs across all eight species investigated. The farer the characteristics are sorted from the origin (and the axes), the more specific is the motif for the respective class of ORs. B, PLS-DA of the data set from (A). The motif qualities are grouped by OR classes. Confidence intervals are color shaded (green, class-I; blue, class-II). As the PC1 axis shows, 20.5% of the total data space contributes to distinguish class-I and class-II OR

consensus across all eight species, each fish OR terminates with a Threonine and a highly conserved Lysine four positions before that ($K_{19}xxxT$), which is part of the $[+]x[+]_{16-20}$ motif. This may suggest at least one *danio rerio*- or fish-specific, C-terminal amino acid motif (Figure S1). Not counting the 133 fish receptors to class-I ORs, however, increased the overall abundance of receptors with at least one motif (>5%) in the remaining 674 class-I ORs to 93.3%.

In the C-termini of both, class-I and class-II ORs, which had an average length of 25 AAs, a single-spaced dibasic [+] x[+] motif ([+] refers to basic AA "R" or "K," and Φ refers to hydrophobic AA "L", "F," "I," "V," or "M" according to [61]) at position C-term$_{3-5}$ after $Y_{7.53}$ appeared to be the most
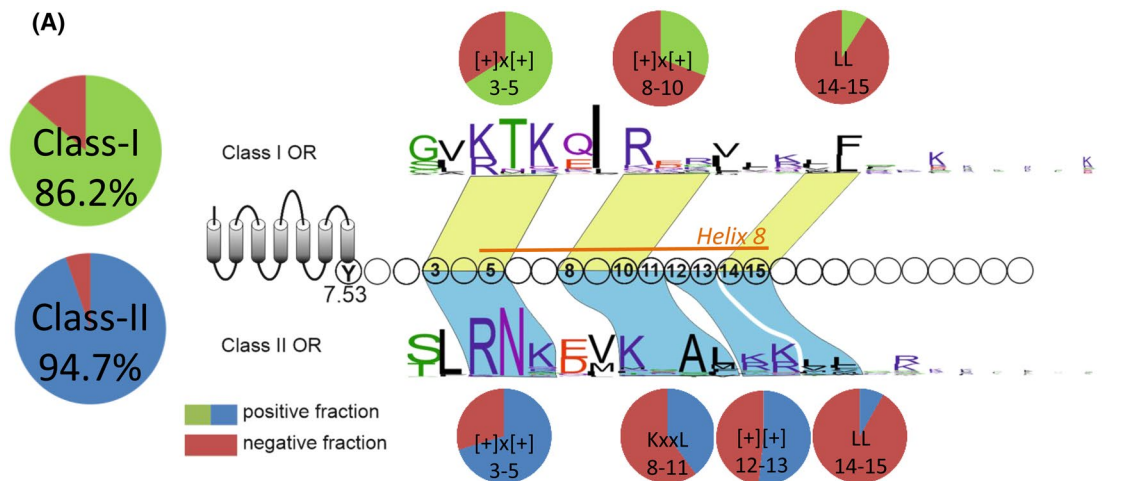
abundant motif (Figure 2A, Table 3). Without counting fish receptors, also the fraction of class-I ORs carrying $[+]x[+]_{3-5}$, $[+]x[+]_{8-10}$, or LL_{14-15} increased to 79.08%, 34.87%, or 10.68%, respectively.

Historically, the "KDEL" motif is one of the earliest identified C-terminal ER retention motifs in proteins.[62] We found this motif ("KD/ExL") in 8.65% of class-II ORs at C-term$_{8-11}$ (Table 3).

We observed, however, conservative AA changes within the conserved C-terminal motifs of the large and heterogeneous group of ORs. For example, the single-spaced dibasic motif at C-term$_{3-5}$ is largely represented as "KxK" in class-I ORs, and as "RxK" in class-II ORs (Figure 2A,B). In class-I
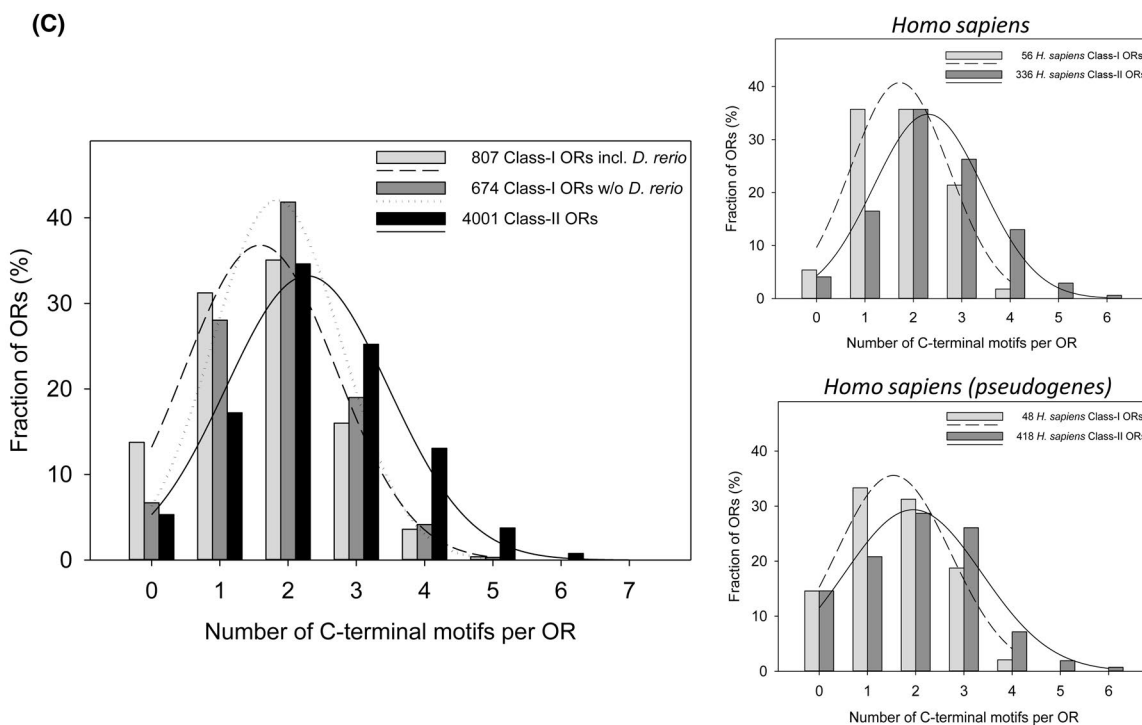
ORs, the motif at C-term$_{3-5}$ is followed by yet another single-spaced dibasic [+]x[+] motif at C-term$_{8-10}$. In class-II ORs, however, the "KD/ExL" motif at C-term$_{8-11}$ is largely replaced by a conserved "KxxL" motif at the same position (Table 3), directly followed by a dibasic [+][+] motif at C-term$_{12-13}$. A typical di-Leucine motif, as described in several nonolfactory GPCRs and other proteins (Table 2) is largely replaced by a degenerate hydrophobic "[Φ][Φ]" motif

FIGURE 2 Class-specific, conserved C-terminal motifs in ORs. A, Large cake diagrams showing the fraction of ORs containing at least one of the known C-terminal motifs involved in intracellular protein transport, as listed in Table 1, at rates >5%, for 807 class-I ORs (green) and 4001 class-II ORs (blue) from eight species. The small cake diagrams represent the fraction of ORs containing a respective C-terminal motif at a given position (numbers given in Table 3). Motifs indicated on the schematic C-terminus extending the snake diagram of a prototypical OR, starting after Y7.53, with an average length of 25 AAs, overlap with GPCR-typical helix 8 (C-term$_{5-15}$). The letters represent an AA sequence logo of the C-terminal region of class-I (top layer) and class-II (bottom layer) ORs, with the size of the letters reflecting the relative frequency of C-terminal AAs across all species investigated. B, C-terminal domains of 1 class-I model OR (OR51E1) and 3 class-II human model ORs as well as 1 class-II murine OR from this study, and five nonolfactory GPCRs, including their identified motifs highlighted in bold letters: black, membrane-proximal OR motifs identified in this study; blue, membrane-proximal GPCR motifs involved in ER export/anterograde trafficking; red, membrane-distal GPCR motifs involved in ER retention/retrograde trafficking (see Tables 1 and 2). C, Distribution of C-termini carrying increasing numbers of positional distinct AA motifs (see Table 3) of class-I ORs from eight species including zebrafish ORs, class-I ORs w/o zebrafish ORs, and class-II ORs. Upper right panel indicates the distribution of numbers of C-terminal motifs per class-I and class-II human ORs, and lower right panel indicates the distribution for human OR pseudogene-deduced amino acid sequences. Curves represent 3-parameter Gaussian fits to the data

at C-term$_{14-15}$, with abundancies of 55.5% or 49.6% in class-I or class-II ORs, respectively (Figure 2A,B). Other identified degenerate C-terminal motifs with abundancies >5% across all species are listed in Table 3.

Figure 2B depicts two class-II model ORs, which have C-terminal sequences matching at least the consensus sequence of motifs at C-term$_{3-5}$, C-term$_{8-11}$, C-term$_{12-13}$, and C-term$_{14-15}$ as identified in our in silico analysis (Figure 2B), and for which validated agonists are available: OR8D1/sotolone,[8] and OR1A1/(R)-(-)-carvone.[1,63] Here, Alanine scanning mutations within the consensus sequence of the identified motifs in OR8D1 and OR1A1 may lead to loss-of-function OR phenotypes with respect to plasma membrane expression and/or signaling. In contrast, two further class-II ORs with validated agonists already deviate from the consensus sequence of specific motifs identified: OR2M3 (agonist: 3-mercapto-2-methylpentanol[5]) deviates from the KxxL motif at C-term$_{8-11}$, and mouse receptor Olfr16 (agonist: lyral[64]) deviates from a dibasic [+][+] motif at C-term$_{12-13}$, and the di-Leucine motif at C-term$_{14-15}$ (Figure 2B). Restoring the consensus sequence of deviating motifs in these two receptors may, thus, rescue their plasma membrane expression and/or signaling, leading to gain-of-function OR phenotypes. Finally, OR51E1 (agonist: butyric acid[8]) served as a model receptor for class-I ORs, since its C-terminus matches the consensus sequence of the identified motifs at C-term$_{3-5}$, C-term$_{8-10}$, and C-term$_{14-15}$ (Figure 2B).

Aligning the C-termini of six nonolfactory GPCRs, for which functional C-terminal trafficking signals have been reported, with the C-termini of the five model ORs in our study, revealed that the dibasic ER retention signals in GPR15, GABBR1a, and TAS1R2 consistently locate membrane-distal at positions >C-term$_{23}$, which is beyond the positions of all C-terminal motifs we identified in ORs (Figure 2B, red-colored motifs, see also Table 1). We may, thus, define all motifs in ORs located at consensus positions <C-term$_{21}$, as identified in this study, as membrane-proximal. Notably, the anterograde trafficking motifs of nonolfactory GPCRs, however, consistently locate membrane-proximal within C-term$_{2-15}$, overlapping

with the C-terminal region in which we identified most motifs in ORs (Figure 2B, blue-colored motifs, see also Table 2). For example, the dibasic anterograde trafficking motif of GPR15 co-locates with the first position of the motifs at C-term$_{8-10}$ and C-term$_{8-11}$ of class-I and class-II ORs, respectively. Similarly, the di-Leucine anterograde trafficking motif of Drd1, ADRB2, and AVPR2 overlap or co-localize with the di-Leucine motif at C-term$_{14-15}$ in ORs (Figure 2B). This suggests that the motifs we identified in ORs may rather promote their plasma membrane expression and signaling.

Calculating the number of identified C-terminal motifs per OR across all 4808 receptors investigated revealed two major findings: 1. ORs can be individually equipped with up to seven out of the eight C-terminal motifs we identified in this study per receptor, and 2. The mean number of C-terminal motifs per receptor is significantly lower in 807 class-I ORs as compared to 4001 class-II ORs (z-test, $z = -17.51$, $P < .05$). For example, any class-I or class-II OR is equipped, on average, with 1.59 ± 1.11 or 2.28 ± 1.19 of such motifs, respectively (Figure 2C). Excluding fish receptors from class-I ORs, however, shifts their Gaussian distribution to the right, yielding an average number of C-terminal motifs per receptor of 1.83 ± 0.94 in the remaining 674 class-I ORs (Figure 2C, Supplemental material, Mendeley Data, V1, https://doi.org/10.17632/49n4t7b4r2.1), which still is significantly different to class-II ORs (z-test, $z = -12.33$, $P < .05$). Similarly, in humans, the mean number of C-terminal motifs per receptor is significantly lower in 56 class-I ORs as compared to 336 class-II ORs (z-test, $z = -4.41$, $P < .05$). For example, any human class-I or class-II OR is equipped, on average, with 1.79 ± 0.91 or 2.39 ± 1.16 of C-terminal motifs per receptor, respectively (Figure 2C, upper right panel). Notably, we obtained similar numbers when analyzing the C-terminal motifs in the amino acid sequences deduced from human OR pseudogenes. Again, the mean number of C-terminal motifs per pseudogene-deduced OR sequence is significantly lower in 48 class-I sequences as compared to 421 class-II sequences (z-test, $z = -2.31$, $P < .05$). For example, any human class-I or class-II pseudogene-deduced OR is equipped, on average,

TABLE 3 Abundance of C-terminal motifs in ORs

Motif	Position	Class-I ORs with motif (%)	Class-I ORs (w/o *D. rerio*) with motif (%)	OR51E1 with motif	Class-II ORs with motif (%)	OR8D1 with motif
[+]x[+]	3-5	66.1	79.8	KxK	70.3	RxK
[+][+]	8-9	10.7	12.8	-	8.9	-
[+]x[+]	8-10	30.9	34.9	RxR	-	-
KD/ExL	8-11	-	-	-	8.6	-
KxxL	8-11	-	-	-	39.9	KKAL
[+][+]	12-13	6.4	7.7	-	51.7	RK
LL	14-15	8.9	10.7	-	8.2	-
[+]x[+]	13-16	5.1	-	-	7.2	-
[+][+]	16-20	25.3	27.5	-	28.5	-
[+]x[+]	16-20	12.3	14.2	-	14.6	-

Note: [+], basic AAs considered: R, K. -, not applicable.

with 1.60 ± 1.03 or 1.98 ± 1.28 of C-terminal motifs per receptor, respectively (Figure 2C, lower right panel).

The most pronounced separation of class-I and -II ORs (z-test, $z = -4.77$, $P < .05$), with respect to their number of C-terminal motifs per receptor, we found in Platypus (oa)—here, class-II ORs harbor, on average, about one additional C-terminal motif per receptor, with 1.53 ± 1.04 or 2.38 ± 1.27 of C-terminal motifs per class-I or class-II OR, respectively (Figure S2).

3.2 | The numbers of C-terminal motifs in ORs increased with evolution
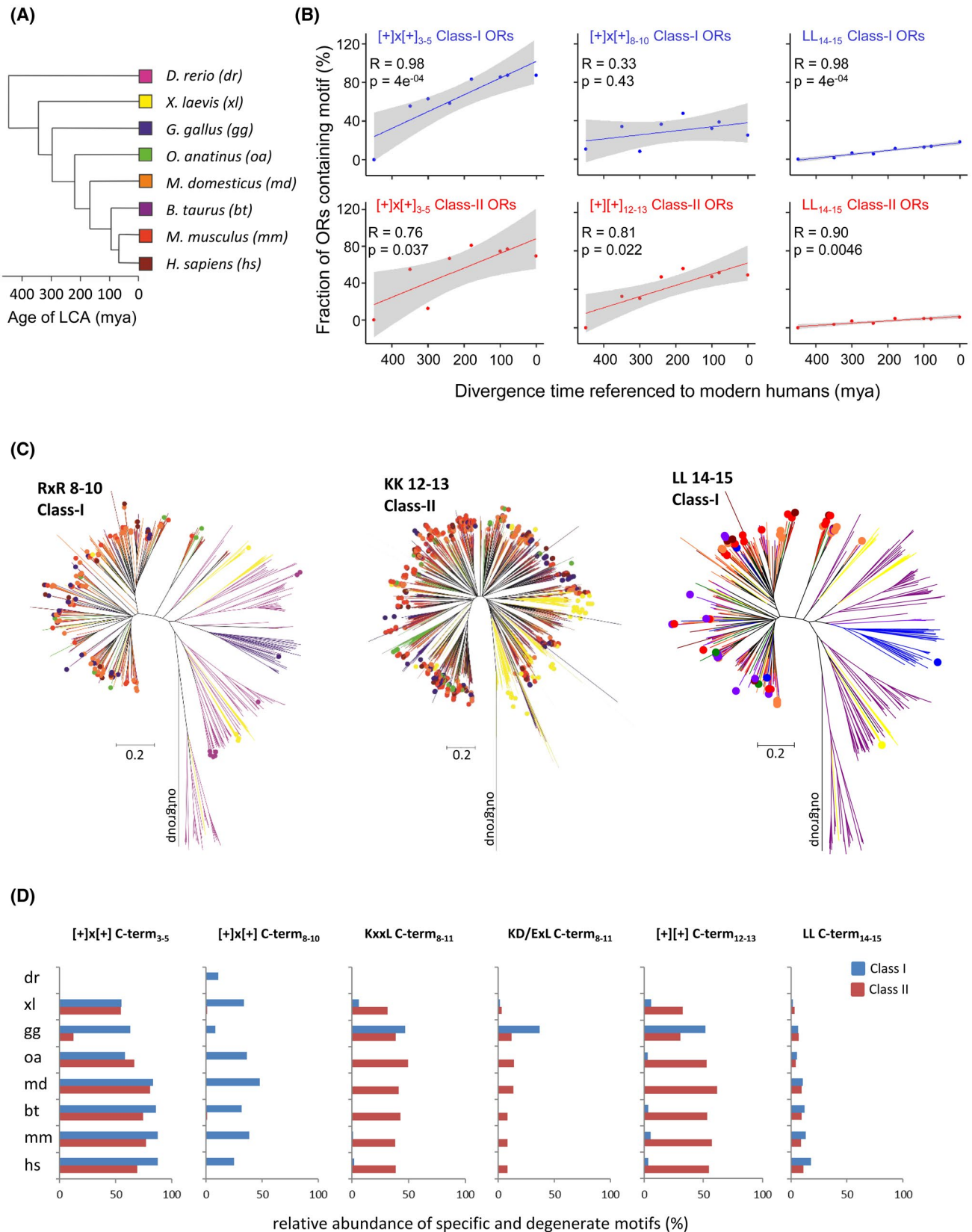
C-terminal motifs in ORs appear to have accumulated with proceeding evolution, that is, the relative abundance of many motifs increased from zebrafish, or at least frog to human (Figure 3A,B). This increase typically is linear and shows a significant Spearman correlation, for example, in class-I ORs: "[+]x[+]" (C-term$_{3-5}$; $R = 0.98$), and "LL" (C-term$_{14-15}$; $R = 0.98$), with the exception of "[+]x[+]" (C-term$_{8-10}$; $R = 0.33$). Likewise, we observed a significant Spearman correlation in class-II ORs: "[+]x[+]" (C-term$_{3-5}$; $R = 0.76$), "[+][+]" (C-term$_{12,13}$ $R = 0.81$), and "LL" (C-term$_{14,15}$; $R = 0.90$) (Figure 3B). Here, chicken appears to be an outlier with respect to the "[+]x[+]" motifs in both, class-I ORs at C-term$_{8-10}$, and class-II ORs at C-term$_{3-5}$. We therefore also analyzed the evolutionary accumulation of certain motifs not only on the species level, but also on the level of individual ORs. We calculated phylogenetic, rooted trees, using the prototypic GPCR rhodopsin as out-group, for all investigated ORs across species, exemplarily tagged according to the presence of, for example, class-I or class-II-differentiating C-terminal motifs, such as "RxR" (C-term$_{8-10}$) or "KK" (C-term$_{12,13}$) (Figure 3C). ORs containing one of these motifs appear more frequently in recent clades, mainly in mammalian OR. This effect was independent of the actual size of the respective species' OR repertoire, and became even more pronounced using degenerate motifs (Figure 3D).

3.3 | C-terminal truncations <C-term$_{15}$ abolished the functional membrane expression of class-II model odorant receptor OR8D1

To improve their functional expression in test cell systems, empirically, recombinant ORs have been N-terminally extended by protein tags to facilitate their transport to the cell surface.[47,65,66] Moreover, odorant-induced signaling of ORs critically depends on the presence of the olfactory Gα_{olf} protein,[7] and, at least in part, on the presence of certain chaperones.[26,27,29] Consequently, improved test cell systems have

been developed, co-expressing N-terminal tag-extended ORs with the olfactory G protein alpha subunit (GNAL), accessory proteins, chaperones, and reporter enzymes, enabling the de-orphaning of ORs,[47,67] and the quantification of their cell surface expression.[47] Here, we used HaloTag-IL-6-tagged ORs to monitor their odorant-induced signaling with

FIGURE 3 The numbers of C-terminal motifs in ORs increased with evolution. A, Phylogenetic relationship among species investigated. Nodes reflect the split times (LCA, last common ancestor; mya, million years ago). B, Regression analyses of the fraction of ORs harboring a respective motif over the phylogeny of the eight species investigated, for class-I ORs (upper panel) and class-II ORs (lower panel). Divergence time is referenced to modern humans (−0.4 mya) and according to the age of LCA in subpanel A. C, Phylogenetic reconstruction across all investigated species, color coded according to subpanel (A), of the evolutionary relationships of ORs carrying specific C-terminal motifs. Class-specific, rooted, phylogenetic trees are based on AA sequences for class-I and class-II ORs. All ORs fitted with the indicated C-terminal motif are marked with a dot of respective species' color. D, Fraction of ORs with the specific motifs from subpanel (C), or the respective degenerate motifs in class-I (blue) and class-II ORs (red)

the cAMP GloSensor assay,[47] and their cell surface expression by flow cytometry (Figure 4A,B).

A direct and indirect involvement of the intracellular C-terminus for translocation to the plasma membrane and signaling of different GPCRs is widely accepted (Table 2). Research on the function of intracellular domains of ORs, so far, mainly investigated the "MAYDRY" motif at the transition of transmembrane domain 3 (TM3) and intracellular loop 2 (ICL2), which in ORs and other GPCRs regulates the interaction with heterotrimeric G proteins.[68–70]

In a model receptor, OR8D1, which has C-terminal motifs close to the consensus sequence for class-II ORs (Figure 4C), we truncated the relatively short C-terminus of OR8D1 (18 AA) stepwise, according to the class-II OR motifs at $C\text{-term}_{3-5}$, $C\text{-term}_{8-11}$, and $C\text{-term}_{12-15}$ (Table 3, Figure 4C). We tested the OR8D1 truncations in a heterologous expression system (see Figure 4A,B) with its ligand sotolone (3-hydroxy-4,5-dimethylfuran-2(5H)-one) [8] (Figure 4C,D). Truncating the C-terminal three AA ($\Delta C\text{-term}_{16-18}$) resulted in a marked reduction (~40%) of both surface expression and cAMP signaling efficacy, and in a significantly increased EC_{50}, as compared to OR8D1 wild-type (wt) (Figure 4C,D, Table S16). All further stepwise truncations ($\Delta C\text{-term}_{12-18}$, $\Delta C\text{-term}_{8-18}$, $\Delta C\text{-term}_{3-18}$) resulted in a complete loss-of-function of these three mutants (Figure 4C), with a significantly reduced surface expression to on average $20.58 \pm 0.11\%$ relative to OR8D1 wt (Figure 4D, dashed line).

3.4 | A membrane-proximal, conserved, single-spaced dibasic C-terminal motif in ORs is necessary for receptor signaling
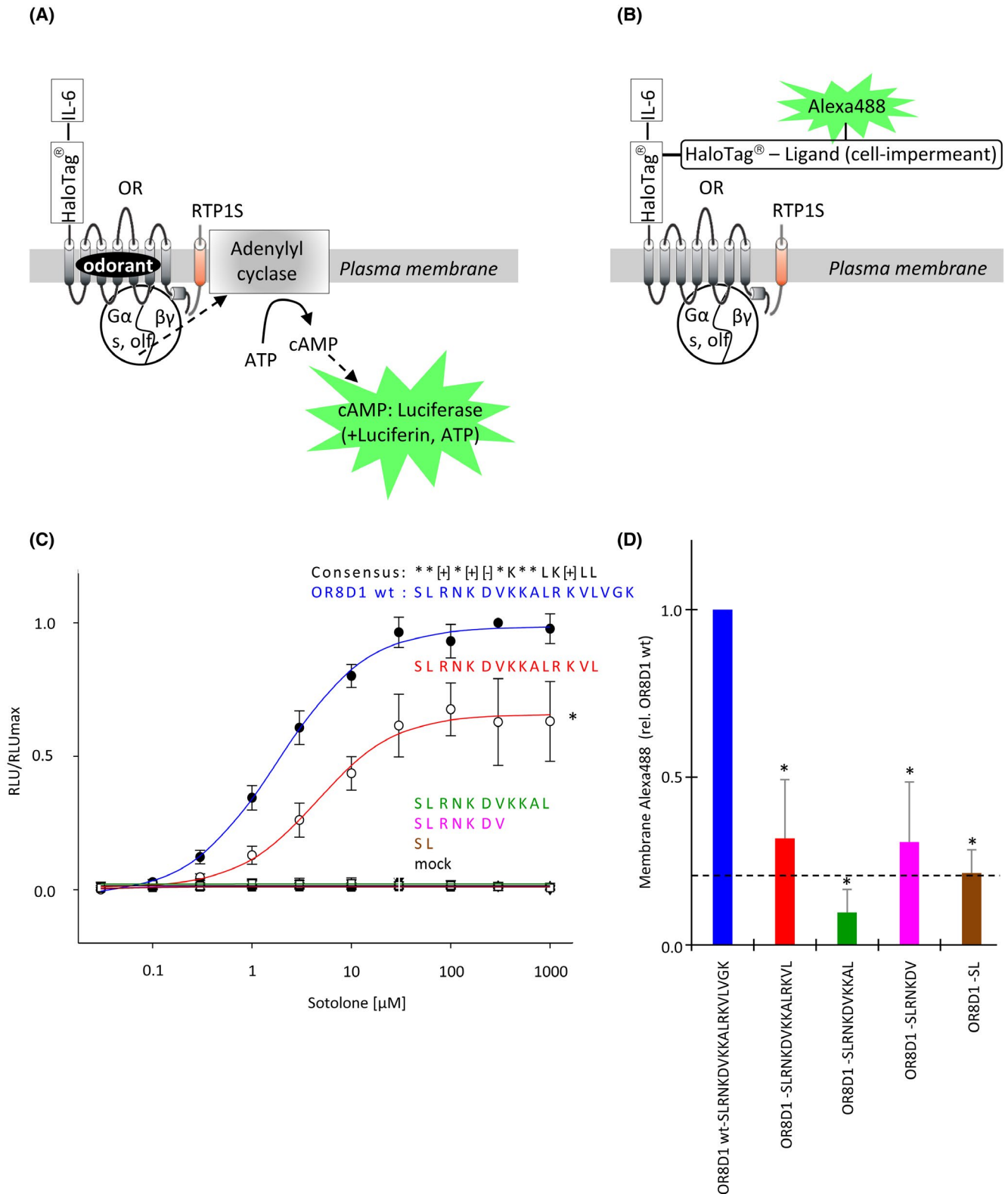
Our in silico analyses revealed that the conserved C-terminal motifs we identified in ORs exclusively overlap with similar, membrane-proximal motifs in the C-termini of nonolfactory GPCRs, which have been demonstrated to support their anterograde trafficking and functional expression (Figure 1B). We therefore predicted that any mutation leading to a nonconservative deviation from the consensus sequence of highly conserved, C-terminal motifs in ORs would lead to loss-of-function phenotypes. Since C-terminal truncations of OR8D1, deleting the conserved, consensus class-II OR motifs at $C\text{-term}_{3-5}$, $C\text{-term}_{8-11}$, and $C\text{-term}_{12-15}$, revealed

their importance for a functional membrane expression, we systematically exchanged AAs within these motifs by site-directed mutation. We then performed functional experiments with all mutants of four selected human wt receptors, OR51E1 (class-I), OR1A1, OR2M3, and OR8D1 (all class-II), and the murine receptor Olfr16 (class-II), and their respective agonists (Table S16-S20). First, we focused on the quantitatively most dominant, single-spaced dibasic motif at membrane-proximal position $C\text{-term}_{3-5}$.
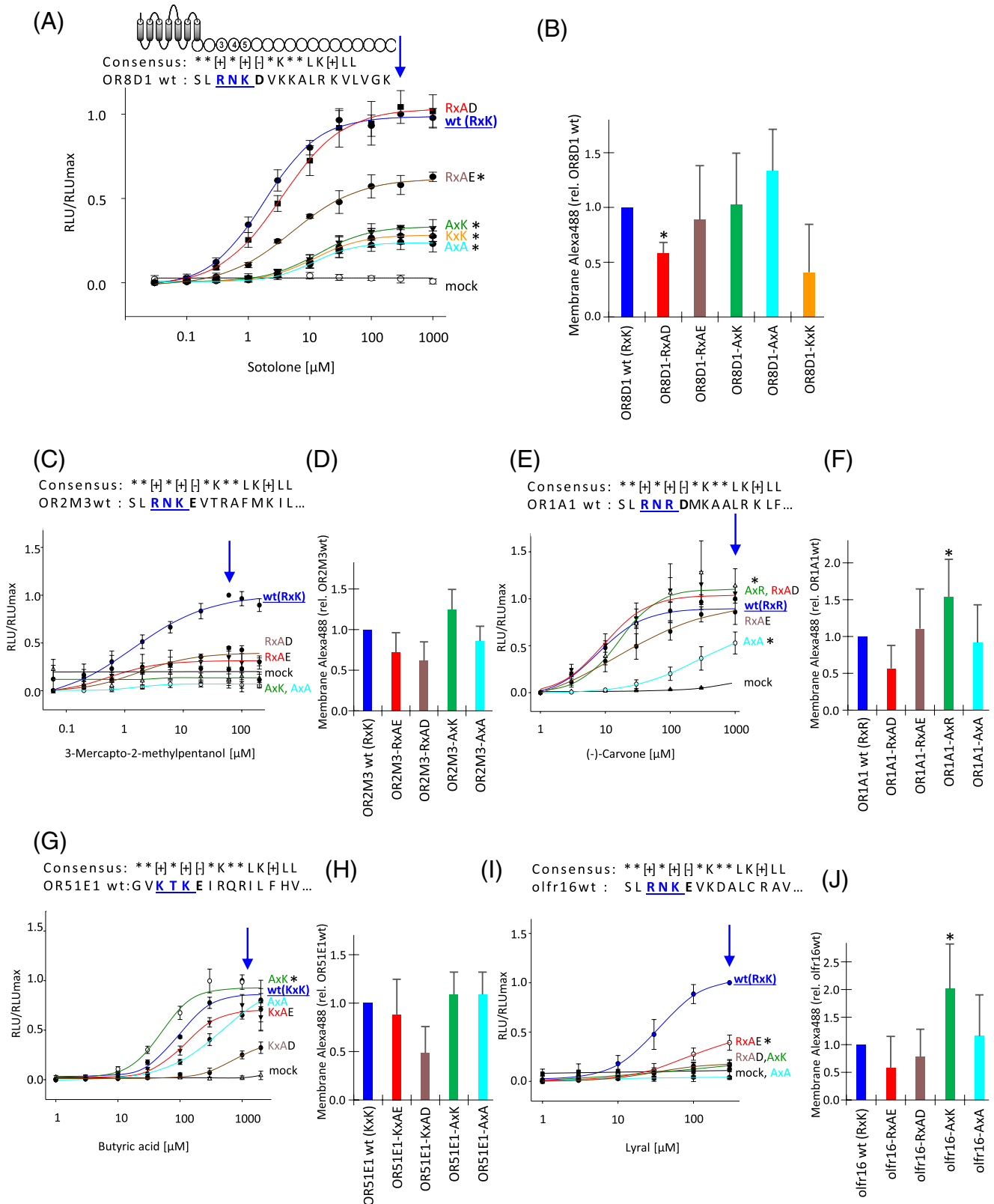
In OR8D1, exchanging either the Arginine of the "RxK" motif at $C\text{-term}_{3-5}$, or both basic AA to an Alanine, reduced the cAMP signaling efficacy about threefold and increased the EC_{50} sixfold, without affecting cell surface expression of these mutants (Figure 5A,B, Table S16). Replacing the Arginine at $C\text{-term}_3$ to a Lysine not only had a similar effect on the efficacy, but also significantly reduced membrane expression. Replacing the Lysine at $C\text{-term}_5$ by an Alanine did neither change the efficacy, nor the EC_{50} (Figure 5A), but attenuated cell surface expression significantly (Figure 5B). However, additionally exchanging the adjacent Aspartate at $C\text{-term}_6$ to a Glutamate reduced the efficacy by half, without changing the EC_{50} (Figure 5A, Table S16).

Together, these results suggest an important role of the single-spaced, dibasic "RxK" motif at $C\text{-term}_{3-5}$ in the class-II receptor OR8D1 for signaling. Having a class-I-exclusive Lysine at $C\text{-term}_3$, or a conservative exchange of the acidic residue adjacent to $C\text{-term}_5$, however, may affect this class-II OR's membrane expression as well.

We observed similar effects in four other receptors. Single Alanine mutation of either of the basic residues at $C\text{-term}_{3-5}$, or of both, mainly affected odorant-induced cAMP signaling of ORs. Exchange of the basic residue at $C\text{-term}_3$ into an Alanine never attenuated (Figure 5B,D,H), but rather increased surface expression of an OR significantly (Figure 5F,J). In general, we observed a significantly diminished cell surface expression of mutant ORs only in some cases where we changed the second basic residue at $C\text{-term}_5$ to an Alanine. In any case, however, mutations in $C\text{-term}_{3-5}$ never decreased cell surface expression significantly below 50%, as compared to the respective wild-type OR (Figure 5B,D,F,H,J, compare to Figure 4D), demonstrating a general lack of congruency of any mutation-induced effects on cell surface expression with effects on signaling of the respective ORs.

FIGURE 4 Truncations suggest the prototypical C-terminus of OR8D1 to be necessary for cell surface expression and cAMP signaling. A, Schematic of the cellular assay system with the cAMP-sensitive luciferase-based GloSensor, activated by odorant/receptor-induced cAMP signaling. B, Schematic of the cellular flow cytometry assay, using cell-impermeant, Alexa 488-labeled HaloTag ligand for the fluorometric detection of cell surface-expressed recombinant ORs and their mutants. C, Concentration-response curves of OR8D1 and its C-terminal truncated variants, as determined by the assay system in (A). C-terminal AAs are depicted as single letter code. D, Bar chart showing the relative surface expression of C-terminally truncated OR8D1 variants, using the flow cytometry assay in (B). Asterisks indicate statistically significant effects on EC_{50} (compare Table S16) as identified by a paired t test, with $P < .05$

FIGURE 5 Mutations in C-term$_{3-5}$ of ORs mainly affected odorant-induced signaling. A, C, E, G, I, odorant concentration-cAMP-response relations for OR8D1, OR2M3, OR1A1, OR51E1, mouse Olfr16, and their mutants, respectively. The blue arrows indicate the concentration measured against the respective odorant receptor, to which we normalized all data of this odorant receptor. B, D, F, H, J, relative surface expression of OR8D1, OR2M3, OR1A1, OR51E1, mouse Olfr16, and their mutants, respectively. Asterisks indicate statistically significant effects on EC$_{50}$ compared to wt (Tables S16-S20) as identified by a paired t test, with $P < .05$

FIGURE 6 Mutations in C-term$_{8-15}$ of ORs affected their surface expression and odorant-induced signaling. A, B, OR8D1/sotolone; C, OR2M3/3-mercapto-2-methylpentanol; **D**, OR1A1/(-)-carvone; E, Olfr16/lyral, and their respective mutants. Blue bars represent relative (to wt) cAMP luminescence, in response to odorant concentrations eliciting maximum effect in concentration-response relations from each wt OR and its specific ligand (Figures S3-S6). Red bars represent surface expression of ORs and their mutants, relative to their respective wt receptor. Asterisks indicate statistically significant effects as compared to the wt, identified by a paired t test, with $P < .05$

Altogether, the study around the dibasic motif at C-term$_{3-5}$ as presented in Figure 5 suggested its crucial role in odorant-induced and receptor-mediated signaling.

3.5 | Key residues in conserved C-terminal motifs 8-11 and 12-15 are necessary for signaling and surface expression, respectively

From our in silico analyses, we predicted that mutations leading to nonconservative AA changes deviating from the consensus sequence of highly conserved C-terminal motifs in ORs would lead to loss-of-function phenotypes. For OR8D1 and three other class-II ORs, we therefore interrogated the role of key residues within conserved motifs further into the C-terminus, at C-term$_{8-11}$, C-term$_{12-13}$, and C-term$_{14-15}$, by mutational analysis and by measuring cAMP signaling and cell surface expression of wt and mutant receptors.

In OR8D1, within C-term$_{8-11}$, both the Lysine at position 8 as well as the Leucine at position 11 were necessary for a functional expression of the receptor (Figure 6A). Mutating either of these two positions, or both, resulted in a significant loss of cell surface expression, alongside with a significantly diminished cAMP signaling (Figure 6A). Moreover, introducing a hydrophobic residue (Leucine, L) at C-terminal position 10, replacing the highly conserved consensus Alanine, decreased cell surface expression significantly below 50%, as compared to the wt receptor. We observed the strongest effects when introducing a Leucine at C-term$_{10}$, which in combination with mutating the Lysine at C-term$_8$ abolished cAMP signaling completely (Figure 6A). We observed similar results in three other class-II ORs (Figure 6C-E).

Vice versa, from our in silico analyses, we predicted that restoring a consensus-like sequence in consensus-deviating C-terminal motifs of model receptors OR2M3 and Olfr16 would lead to gain-of-function phenotypes. In fact, changing in OR2M3 wt the "TxxF" motif at C-term$_{8-11}$, which deviates from the consensus sequence, back to a consensus-like "KxxL" motif, increased the cell surface expression significantly, as predicted, and yielded a fourfold gain-of-function in cAMP signaling (Figure 6C).

Mutating residues within C-term$_{12-13}$ or C-term$_{14-15}$ in OR8D1 to Alanine resulted in a diminished cell surface expression and cAMP signaling, which was significant when just mutating the first basic and second hydrophobic residues, at C-terminal positions 8 and 11, respectively (Figure 6B). Cell surface expression and cAMP signaling dropped to 50% when mutating each position of OR8D1 C-term$_{12-15}$ to Alanine (Figure 6B). Vice versa, and as predicted, changing the consensus-deviating motifs at C-term$_{12-13}$ or C-term$_{14-15}$ in human OR2M3 ("MKIL") or mouse Olfr16 ("CRAV") back to a consensus-like "K^{+}LL" motif, increased the

cell surface expression of both receptors significantly and yielded a 2.5 to 4-fold gain-of-function in cAMP signaling (Figure 6C,E).

Altogether, the mutational experiments with motifs C-term$_{8-11}$, C-term$_{12-13}$, and C-term$_{14-15}$ suggested a role of C-term$_{8-11}$ of ORs rather for signaling, whereas the motifs at C-term$_{12-13}$ and C-term$_{14-15}$ appeared to be involved rather in cell surface expression, with secondary effects on signaling (Figure 6B-E).

4 | DISCUSSION

In the present study, by large-scale in silico analyses of ORs from different species, we unambiguously demonstrate the existence of highly conserved C-terminal amino acid motifs.

The C-terminal motifs of ORs identified in this study largely overlap with amphipathic helix 8,[43,44] which in a variety of GPCRs has been shown to be involved in G protein coupling, receptor dimerization, interaction with the plasma membrane, and internalization.[71–76] The motifs we identified are also well known in nonolfactory GPCRs and other proteins, where they have been identified as sites of protein-protein interactions, for instance in the context of intracellular transport mechanisms, for example, ER retention/retrieval, or ER export/plasma membrane translocation, and may be located at membrane-distal and -proximal sites, with different functional implications.[32,35,77,78] The overall location of motifs we identified in ORs in the present study exclusively co-localize or overlap with membrane-proximal C-terminal motifs in nonolfactory GPCRs that have been functionally validated to rather support anterograde trafficking and/or signaling of receptors. According to our in silico analyses-based prediction, all our Alanine mutation scans with motifs matching the consensus sequence resulted in loss-of-function phenotypes of the respective ORs. Vice versa, and as predicted, restoring a consensus-like sequence in the consensus-deviating C-terminal motifs of OR2M3 and Olfr16 resulted in gain-of-function receptor phenotypes with respect to both plasma membrane expression and signaling, suggesting that conserved C-terminal motifs in ORs rather are necessary for their anterograde trafficking and functional expression, at least in test cell systems. Detrimental effects of deviating from an OR-consensus at 66 critical sites on mouse ORs' surface expression in a most recent study, suggested that an intracellular retention of ORs may be caused by their overall structural instability.[38] In their study, Ikegami et al. (2020) did not, however, identify any conserved C-terminal motifs, associated, for instance, with anterograde trafficking of ORs. However, three of the four C-terminal, "critical OR consensus sites" identified by Ikegami et al. (2020) (C-term$_{11}$, C-term$_{13-14}$) overlap with the consensus-like motifs "KxxL" (C-term$_{8-11}$), and "K^{+}LL" (C-term$_{12-15}$) identified in our study.

ORs harbor the most conserved and most membrane-proximal C-terminal, spaced dibasic "[+]x[+]" motif at C-term$_{3-5}$ (see also Ref. 31). Our observation that an Alanine mutation of the basic residue at C-term$_3$ never attenuated the surface expression of the ORs investigated is in line with reports showing that a membrane-proximal, dibasic "[+]x[+]" motif may not be accessible for any intracellular transport mechanisms.[32,35,78] In contrast, Alanine mutation of the most proximal or both basic residues at C-term$_{3-5}$, or a C-terminal truncation that deleted C-term$_{3-5}$ in OR8D1, significantly diminished or abolished cAMP signaling of the ORs investigated in our study, suggesting their involvement in G protein coupling and signaling, as demonstrated previously for intracellular, membrane-proximal residues within GPCRs[76,79,80] or ORs.[43,44] For instance, truncation experiments in the rat melanin-concentrating hormone receptor Mch1r, which deleted a membrane-proximal, dibasic "RxR" motif in amphiphilic helix 8, abolished G protein signaling of this receptor.[76] In the class-II mouse OR Olfr73 (mOR-EG, MOR174-9), a C-terminal truncation of 12 AA abolished receptor function,[81] presumably because this truncation deleted the motif at C-term$_{12-15}$ ("KKLL") as well as the last hydrophobic residue of motif C-term$_{8-11}$ ("KxxL"). This goes along well with our findings from the truncation experiments and mutational scans with OR8D1 and three other ORs, showing that both motifs are important for surface expression and signaling of ORs.

Furthermore, the amino acid environment may influence the respective motif's strength. Our findings that the quality of the N-terminal acidic residue of the cytosolic helix 8 at C-term$_6$, adjacent to the "RxR" motif of OR8D1 at C-term$_{3-5}$, affected signaling, is in line with a report by Kawasaki et al. (2015) who demonstrated this residue to be involved in G protein signaling of mouse OR Olfr544 (mOR-S6).[43] Ikegami et al. (2020) have also pointed out this position as a critical consensus position important for an overall structural stability of ORs.[38] Similarly, a Glutamate at a homologous position in human vasopressin V2 receptor (AVPR2), in connection with a C-terminal di-Leucine motif homologous with C-term$_{10-11}$ of motif C-term$_{8-11}$ ("KxxL") in ORs, affected cell surface expression of AVPR2.[82] Furthermore, future experiments may reveal the impact of the highly conserved Threonine or Asparagine within dibasic "[+]x[+]" motif at C-term$_{3-5}$, in class-I ORs or class-II ORs, respectively, or of the highly conserved Alanine at C-term$_{10}$ within the "KxxL" motif at C-term$_{8-11}$ in class-II ORs.

The C-terminal consensus of *danio rerio* sequences deviates from the consensus across eight species in our study. The presence of a highly conserved, C-terminal "KxxxT" motif in *danio rerio* suggests that fish ORs may have evolved with C-terminal amino acid motifs deviating from the mammalian-biased motifs as summarized in Tables 1 and 2. This warrants an investigation of other fish phylogenetic clades, which

may lead to the discovery of further fish-typical, C-terminal motifs.

In addition to C-terminal motifs, non-C-terminal intracellular domains in GPCRs may contain conserved, dibasic motifs, such as the "RxR" motif, which may function as an ER retention/retrieval signal in certain GPCRs.[83] A similar motif in ORs, besides the highly conserved motif at C-term$_{3-5}$, can be found, for instance, in ICL3$_{15-17}$, with rates of 63.6% and 76.3% in class-I and class-II ORs, respectively, and "RxK" being the most abundant motif in either class (MK, DK, unpublished observations). Moreover, distinct motifs within the N-terminal domains of GPCRs may regulate their intracellular, anterograde transport,[84–86] which has been demonstrated for ORs, for example, with N-terminal glycosylation sites.[81] Thus, the frequent use of additional N-terminal tags with recombinant ORs, however, may override to a certain degree any effects of their trafficking motifs in test cell systems, making it hard to demonstrate experimentally subtle differences in their individual equipment with certain AA motifs, or even single AA within these motifs.

Here, we identified highly conserved AA motifs that discriminate between class-I and class-II ORs and are instructive for their surface expression and/or signaling. This may suggest the interaction of ORs via these conserved motifs with different chaperones, only some of which may have been identified, so far.[25–29] In a family of mitochondrial TIM chaperone proteins, for example, distinct amino acid motifs have been shown to be maintained in the eukaryote lineage, and have been suggested to provide for a broad range of substrate proteins to be chaperoned to the mitochondrial intermembrane space.[87] From our experiments changing the class-II OR-typical "RxK" motif at C-term$_{3-5}$ in OR8D1 to the class-I OR-typical "KxK" motif, it may be assumed that a rather conservative AA exchange more or less conserves the function of the respective motif, but nevertheless may modulate its effective strength. The occurrence of conservative AA changes within many of the identified motifs, indeed, revealed a certain degenerateness of motifs, a phenomenon, which was previously reported for glycosyltransferases and nonolfactory GPCRs.[30,82,88,89] Such a diversification of motifs, together with the observed increase in the number of different C-terminal motifs with evolution, may be a consequence of growing OR repertoires and a higher demand for regulated intracellular transport and signaling. A higher degree of realizable combinations of different C-terminal motifs, at least within a given receptor class, may enable subtle zip coding, and thus, fine-tuning of ORs' surface expression and cAMP signaling in their respective OSNs.

We may, thus, test whether, hypothetically, there might exist enough possible combinations to equip ORs of an entire receptor repertoire individually with C-terminal motifs, by calculating a maximum number of possible combinations of conserved C-terminal motifs in ORs only on distinct positions, by

using the formula for *k*-permutations of n (selecting k items from a collection of n items, with k ≤ n): $\frac{n!}{(n-k)!}$). If we assume n = 8 positional different motifs (as identified in this study, see Table 3), and conservatively allow any given class-I OR to harbor, on average, up to k = 2 different C-terminal motifs (compare Figure 2C), this would result in 56 combinations. This number of C-terminal motif combinations would allow to individually equip the entire class-I OR repertoires of, for example, human or Platypus (Supplemental material, Mendeley Data, V1, https://doi.org/10.17632/49n4t7b4r2.1). Assuming just one additional C-terminal motif for class-II ORs, thus, would result in 336 combinations. This combinatorial equipment with C-terminal motifs would suffice to cover, for instance, the entire Platypus class-II OR repertoire, and 86% of the human class-II OR repertoire.

At this point, we may speculate on a hypothetical role of at least class-I/class-II-discriminating C-terminal motifs in ORs: OR amino acid sequences and expression levels have been shown to determine axonal coalescence into glomeruli of olfactory sensory neurons in vivo.[90] Moreover, Imai et al. (2006) demonstrated that the axon targeting of OSNs depended on OR-derived intracellular cAMP levels.[69] Indeed, ORs possess individual degrees of constitutive activity in the absence of odorant stimulus.[91] According to Zhang et al (2012), glomerular axonal targeting of ORs is uncoupled from stimulus specificity.[92] Most OSNs expressing class-I ORs have been reported to project their axons to an anterodorsal domain in the mouse olfactory bulb,[93] which supposedly was due to odorant-independent, OR-derived cAMP signaling.[69,91,94] Thus, an individual, combinatorial equipment with C-terminal motifs that control ORs' surface expression and/or a proportional, constitutive cAMP signaling may be instructive at least for a differential axon targeting of OSNs expressing either class-I or class-II ORs. Future experiments with genetically engineered mice may reveal an OR class-specific, C-terminal motif-dependent axon targeting of OSNs.

In summary, here, we have demonstrated the existence of highly conserved C-terminal motifs within ORs that discriminate between class-I and class-II receptors, and play an instructive role in their cell surface expression and cAMP signaling.

ACKNOWLEDGMENTS

CONFLICT OF INTEREST

The authors declare no conflict of interest.

AUTHOR CONTRIBUTIONS

D. Krautwurst and M. Kotthoff designed research; J. Bauer, M. Kotthoff, and F. Haag performed research; M. Kotthoff, J. Bauer, F. Haag, and D. Krautwurst analyzed data; D. Krautwurst, F. Haag, and M. Kotthoff wrote the paper.

ORCID

Matthias Kotthoff https://orcid.org/0000-0001-7963-2921
Franziska Haag https://orcid.org/0000-0003-4210-0475
Dietmar Krautwurst https://orcid.org/0000-0002-3350-8682

REFERENCES

1. Geithe C, Noe F, Kreissl J, Krautwurst D. The broadly tuned odorant receptor OR1A1 is highly selective for 3-methyl-2,4-nonanedione, a key food odorant in aged wines, tea, and other foods. *Chem Senses*. 2017;42(3):181-193.
2. Mainland JD, Li YR, Zhou T, Liu WLL, Matsunami H. Human olfactory receptor responses to odorants. *Sci Data*. 2015;2:150002.
3. Saito H, Chi Q, Zhuang H, Matsunami H, Mainland JD.Odor coding by a Mammalian receptor repertoire. *Sci Signal*. 2009;2(60):ra9.
4. Krautwurst D, Kotthoff M. A hit map-based statistical method to predict best ligands for orphan olfactory receptors: natural key odorants versus "lock picks". *Methods Mol Biol*. 2013;1003:85-97.
5. Noe F, Polster J, Geithe C, Kotthoff M, Schieberle P, Krautwurst D. OR2M3: a highly specific and narrowly tuned human odorant receptor for the sensitive detection of onion key food odorant 3-Mercapto-2-methylpentan-1-ol. *Chem Senses*. 2017;42(3):195-210.
6. Sanz G, Schlegel C, Pernollet JC, Briand L. Comparison of odorant specificity of two human olfactory receptors from different phylogenetic classes and evidence for antagonism. *Chem Senses*. 2005;30(1):69-80.
7. Shirokova E, Schmiedeberg K, Bedner P, et al. Identification of specific ligands for orphan olfactory receptors. G protein-dependent agonism and antagonism of odorants. *J Biol Chem*. 2005;280(12):11807-11815.
8. Adipietro KA, Mainland JD, Matsunami H. Functional evolution of mammalian odorant receptors. *PLoS Genet*. 2012;8(7):e1002821.
9. Gonzalez-Kristeller DC, do Nascimento JB, Galante PA, Malnic B. Identification of agonists for a group of human odorant receptors. *Front Pharmacol*. 2015;6:35.
10. Li S, Ahmed L, Zhang R, et al. Smelling sulfur: Copper and silver regulate the response of human odorant receptor OR2T11 to low-molecular-weight thiols. *J Am Chem Soc*. 2016;138(40):13281-13288.
11. Sato-Akuhara N, Horio N, Kato-Namba A, et al. Ligand specificity and evolution of mammalian musk odor receptors: effect of single receptor deletion on odor detection. *J Neurosci*. 2016;36(16):4482-4491.
12. Peterlin Z, Firestein S, Rogers ME. The state of the art of odorant receptor deorphanization: a report from the orphanage. *J Gen Physiol*. 2014;143(5):527-542.
13. Shirokova E, Raguse JD, Meyerhof W, Krautwurst D. The human vomeronasal type-1 receptor family–detection of volatiles and cAMP signaling in HeLa/Olf cells. *Faseb J*. 2008;22(5):1416-1425.
14. Gimelbrant AA, Haley SL, McClintock TS. Olfactory receptor trafficking involves conserved regulatory steps. *J Biol Chem*. 2001;276(10):7285-7290.

15. Gimelbrant AA, Stoss TD, Landers TM, McClintock TS. Truncation releases olfactory receptors from the endoplasmic reticulum of heterologous cells. *J Neurochem*. 1999;72(6):2301-2311.

16. McClintock TS, Landers TM, Gimelbrant AA, et al. Functional expression of olfactory-adrenergic receptor chimeras and intracellular retention of heterologously expressed olfactory receptors. *Brain Res Mol Brain Res*. 1997;48(2):270-278.

17. McClintock TS, Sammeta N. Trafficking prerogatives of olfactory receptors. *NeuroReport*. 2003;14(12):1547-1552.

18. Lu M, Echeverri F, Moyer BD. Endoplasmic reticulum retention, degradation, and aggregation of olfactory G-protein coupled receptors. *Traffic*. 2003;4(6):416-433.

19. Mainland JD, Keller A, Li YR, et al. The missense of smell: functional variability in the human odorant receptor repertoire. *Nat Neurosci*. 2014;17(1):114-120.

20. Menashe I, Man O, Lancet D, Gilad Y. Different noses for different people. *Nat Genet*. 2003;34(2):143-144.

21. Sharon D, Gilad Y, Glusman G, Khen M, Lancet D, Kalush F. Identification and characterization of coding single-nucleotide polymorphisms within a human olfactory receptor gene cluster. *Gene*. 2000;260(1–2):87-94.

22. Geithe C, Krautwurst D. Chirality matters and SNPs make the difference - genetic variations on enantiomer-specific odorant receptors for carvone. In: Taylor AJ, Mottram DS, eds. *Flavour Science: Proceedings of the XIV Weurman Flavour Research Symposium*. Leicestershire, UK: Context Products Ltd.; 2015:297-302.

23. Jaeger S, McRae J, Bava C, et al. A mendelian trait for olfactory sensitivity affects odor experience and food selection. *Curr Biol*. 2013;23(16):1601-1605.

24. Keller A, Zhuang H, Chi Q, Vosshall LB, Matsunami H. Genetic variation in a human odorant receptor alters odour perception. *Nature*. 2007;449(7161):468-472.

25. Neuhaus EM, Mashukova A, Zhang W, Barbour J, Hatt H. A specific heat shock protein enhances the expression of mammalian olfactory receptor proteins. *Chem Senses*. 2006;31(5):445-452.

26. Saito H, Kubota M, Roberts RW, Chi Q, Matsunami H. RTP family members induce functional expression of mammalian odorant receptors. *Cell*. 2004;119(5):679-691.

27. Von Dannecker LE, Mercadante AF, Malnic B. Ric-8B promotes functional expression of odorant receptors. *Proc Natl Acad Sci U S A*. 2006;103(24):9310-9314.

28. Wu L, Pan YI, Chen G-Q, Matsunami H, Zhuang H. Receptor-transporting protein 1 short (RTP1S) mediates translocation and activation of odorant receptors by acting through multiple steps. *J Biol Chem*. 2012;287(26):22287-22294.

29. Zhuang H, Matsunami H. Synergism of accessory factors in functional expression of mammalian odorant receptors. *J Biol Chem*. 2007;282(20):15284-15293.

30. Bermak JC, Li M, Bullock C, Weingarten P, Zhou QY. Interaction of gamma-COP with a transport motif in the D1 receptor C-terminus. *Eur J Cell Biol*. 2002;81(2):77-85.

31. Okamoto Y, Bernstein JD, Shikano S. Role of C-terminal membrane-proximal basic residues in cell surface trafficking of HIV coreceptor GPR15 protein. *J Biol Chem*. 2013;288(13):9189-9199.

32. Okamoto Y, Shikano S. Phosphorylation-dependent C-terminal binding of 14-3-3 proteins promotes cell surface expression of HIV co-receptor GPR15. *J Biol Chem*. 2011;286(9):7171-7181.

33. Woo CH, Gao C, Yu P, et al. Conserved function of the lysine-based KXD/E motif in Golgi retention for endomembrane proteins among different organisms. *Mol Biol Cell*. 2015;26(23):4280-4293.

34. Margeta-Mitrovic M, Jan YN, Jan LY. A trafficking checkpoint controls GABA(B) receptor heterodimerization. *Neuron*. 2000;27(1):97-106.

35. Gassmann M, Haller C, Stoll Y, et al. The RXR-type endoplasmic reticulum-retention/retrieval signal of GABAB1 requires distant spacing from the membrane to function. *Mol Pharmacol*. 2005;68(1):137-144.

36. Bubnell J, Jamet S, Tomoiaga D, D'Hulst C, Krampis K, Feinstein P. In vitro mutational and bioinformatics analysis of the M71 odorant receptor and its superfamily. *PLoS One*. 2015;10(10):e0141712.

37. Hague C, Uberti MA, Chen Z, et al. Olfactory receptor surface expression is driven by association with the beta2-adrenergic receptor. *Proc Natl Acad Sci U S A*. 2004;101(37):13672-13676.

38. Ikegami K, de March CA, Nagai MH, et al. Structural instability and divergence from conserved residues underlie intracellular retention of mammalian odorant receptors. *Proc Natl Acad Sci U S A*. 2020;117(6):2957-2967.

39. Liu AH, Zhang X, Stolovitzky GA, Califano A, Firestein SJ. Motif-based construction of a functional map for mammalian olfactory receptors. *Genomics*. 2003;81(5):443-456.

40. Samsonova EV, Krause P, Bäck T, IJzerman AP. Characteristic amino acid combinations in olfactory G protein-coupled receptors. *Proteins*. 2007;67(1):154-166.

41. Zozulya S, Echeverri F, Nguyen T. The human olfactory receptor repertoire. *Genome Biol*. 2001;2(6):1-12.

42. Palczewski K, Kumasaka T, Hori T, et al. Crystal structure of rhodopsin: a G protein-coupled receptor. *Science*. 2000;289(5480):739-745.

43. Kawasaki T, Saka T, Mine S, et al. The N-terminal acidic residue of the cytosolic helix 8 of an odorant receptor is responsible for different response dynamics via G-protein. *FEBS Lett*. 2015;589(10):1136-1142.

44. Sato T, Kawasaki T, Mine S, Matsumura H. Functional role of the C-terminal amphipathic helix 8 of olfactory receptors and other G protein-coupled receptors. *Int J Mol Sci*. 2016;17(11):1930.

45. Binkowski B, Fan F, Wood K. Engineered luciferases for molecular sensing in living cells. *Curr Opin Biotechnol*. 2009;20(1):14-18.

46. Hamprecht B, Glaser T, Reiser G, Bayer E, Propst F. Culture and characteristics of hormone-responsive neuroblastoma X glioma hybrid cells. *Methods Enzymol*. 1985;109:316-341.

47. Noe F, Frey T, Fiedler J, Geithe C, Nowak B, Krautwurst D. IL-6–HaloTag® enables life-cell plasma membrane staining, flow cytometry, functional expression, and de-orphaning of recombinant odorant receptors. *J Biol Methods*. 2017;4(4):e81.

48. Noe F, Geithe C, Fiedler J, Krautwurst D. A bi-functional IL-6-HaloTag® as a tool to measure the cell-surface expression of recombinant odorant receptors and to facilitate their activity quantification. *J Biol Methods*. 2017;4:e82.

49. HORDE. *The Human Olfactory Receptor Data Exploratorium (HORDE)*. The Weizmann Institute; 2011. http://bioportal.weizmann.ac.il/HORDE/

50. NCBI. *National Center for Biotechnology Information, Gene Search Tool*. 2011. http://www.ncbi.nlm.nih.gov/gene/

51. Ballesteros JD, Weinstein H. Integrated methods for the construction of three-dimensional models and computational probing of structure-function relations in G protein-coupled receptors. *Methods Neurosci*. 1995;25:366-428.

52. Knudsen B, T Knudsen, M Flensborg, et al. *CLC Main Workbench*. CLCbio; 2011.

53. Tamura K, Peterson D, Peterson N, Stecher G, Nei M, Kumar S. MEGA5: molecular evolutionary genetics analysis using maximum likelihood, evolutionary distance, and maximum parsimony methods. *Mol Biol Evol*. 2011;28(10):2731-2739.

54. Thompson JD, Higgins DG, Gibson TJ. CLUSTAL W: improving the sensitivity of progressive multiple sequence alignment through sequence weighting, position-specific gap penalties and weight matrix choice. *Nucleic Acids Res*. 1994;22(22):4673-4680.

55. Saitou N, Nei M. The neighbor-joining method: a new method for reconstructing phylogenetic trees. *Mol Biol Evol*. 1987;4(4):406-425.

56. Felsenstein J. Confidence limits on phylogenies: An approach using the bootstrap. *Evolution*. 1985;39:783-791.

57. Zuckerkandl E, Pauling L. Evolutionary divergence and convergence in proteins. In: Bryson V, Vogel HJ, eds. *Evolving Genes and Proteins*. Academic Press; 1965:97-166.

58. Crooks GE, Hon G, Chandonia JM, Brenner SE. WebLogo: a sequence logo generator. *Genome Res*. 2004;14(6):1188-1190.

59. Haag F, Ahmed L, Reiss K, Block E, Batista VS, Krautwurst D Copper-mediated thiol potentiation and mutagenesis-guided modeling suggest a highly conserved copper-binding motif in human OR2M3. *Cell Mol Life Sci*. 2020;77:2157-2179.

60. Niimura Y. Olfactory receptor multigene family in vertebrates: from the viewpoint of evolutionary genomics. *Curr Genomics*. 2012;13(2):103-114.

61. Aasland R, Abrams C, Ampe C, et al. Normalization of nomenclature for peptide motifs as ligands of modular protein domains. *FEBS Lett*. 2002;513(1):141-144.

62. Munro S, Pelham HR. A C-terminal signal prevents secretion of luminal ER proteins. *Cell*. 1987;48(5):899-907.

63. Geithe C, Protze J, Kreuchwig F, Krause G, Krautwurst D. Structural determinants of a conserved enantiomer-selective carvone binding pocket in the human odorant receptor OR1A1. *Cell Mol Life Sci*. 2017;74(22):4209-4229.

64. Touhara K, Sengoku S, Inaki K, et al. Functional identification and reconstitution of an odorant receptor in single olfactory neurons. *Proc Natl Acad Sci U S A*. 1999;96(7):4040-4045.

65. Krautwurst D, Yau KW, Reed RR. Identification of ligands for olfactory receptors by functional expression of a receptor library. *Cell*. 1998;95(7):917-926.

66. Shepard BD, Natarajan N, Protzko RJ, Acres OW, Pluznick JL. A cleavable N-terminal signal peptide promotes widespread olfactory receptor surface expression in HEK293T cells. *PLoS One*. 2013;8(7):e68758.

67. Zhuang H, Matsunami H. Evaluating cell-surface expression and measuring activation of mammalian odorant receptors in heterologous cells. *Nat Protoc*. 2008;3(9):1402-1413.

68. Sakmar TP, Franke RR, Khorana HG. Glutamic acid-113 serves as the retinylidene Schiff base counterion in bovine rhodopsin. *Proc Natl Acad Sci U S A*. 1989;86(21):8309-8313.

69. Imai T, Suzuki M, Sakano H. Odorant receptor-derived cAMP signals direct axonal targeting. *Science*. 2006;314(5799):657-661.

70. Scheer A, Fanelli F, Costa T, De Benedetti PG, Cotecchia S. Constitutively active mutants of the alpha 1B-adrenergic receptor: role of highly conserved polar amino acids in receptor activation. *Embo J*. 1996;15(14):3566-3578.

71. Kuwasako K, Kitamura K, Nagata S, Hikosaka T, Kato J. Structure-function analysis of helix 8 of human calcitonin receptor-like receptor within the adrenomedullin 1 receptor. *Peptides*. 2011;32(1):144-149.

72. Bruno A, Costantino G, De Fabritiis G, Pastor M, Selent J. Membrane-sensitive conformational states of helix 8 in the metabotropic Glu2 receptor, a class C GPCR. *PLoS One*. 2012;7(8):e42023.

73. Krishna AG, Menon ST, Terry TJ, Sakmar TP. Evidence that helix 8 of rhodopsin acts as a membrane-dependent conformational switch. *Biochemistry*. 2002;41(26):8298-8309.

74. Knepp AM, Periole X, Marrink SJ, Sakmar TP, Huber T. Rhodopsin forms a dimer with cytoplasmic helix 8 contacts in native membranes. *Biochemistry*. 2012;51(9):1819-1821.

75. Delos Santos NM, Gardner LA, White SW, Bahouth SW. Characterization of the residues in helix 8 of the human beta1-adrenergic receptor that are involved in coupling the receptor to G proteins. *J Biol Chem*. 2006;281(18):12896-12907.

76. Tetsuka M, Saito Y, Imai K, Doi H, Maruyama K. The basic residues in the membrane-proximal C-terminal tail of the rat melanin-concentrating hormone receptor 1 are required for receptor function. *Endocrinology*. 2004;145(8):3712-3723.

77. Shikano S, Coblitz B, Sun H, Li M. Genetic isolation of transport signals directing cell surface expression. *Nat Cell Biol*. 2005;7(10):985-992.

78. Shikano S, Li M. Membrane receptor trafficking: evidence of proximal and distal zones conferred by two independent endoplasmic reticulum localization signals. *Proc Natl Acad Sci U S A*. 2003;100(10):5783-5788.

79. Madabushi S, Gross AK, Philippi A, Meng EC, Wensel TG, Lichtarge O. Evolutionary trace of G protein-coupled receptors reveals clusters of residues that determine global and class-specific functions. *J Biol Chem*. 2004;279(9):8126-8132.

80. Kling RC, Lanig H, Clark T, Gmeiner P. Active-state models of ternary GPCR complexes: determinants of selective receptor-G-protein coupling. *PLoS One*. 2013;8(6):e67244.

81. Katada S, Tanaka M, Touhara K. Structural determinants for membrane trafficking and G protein selectivity of a mouse olfactory receptor. *J Neurochem*. 2004;90(6):1453-1463.

82. Schulein R, Hermosilla R, Oksche A, et al. A dileucine sequence and an upstream glutamate residue in the intracellular carboxyl terminus of the vasopressin V2 receptor are essential for cell surface transport in COS.M6 cells. *Mol Pharmacol*. 1998;54(3):525-535.

83. Hermosilla R, Schulein R. Sorting functions of the individual cytoplasmic domains of the G protein-coupled vasopressin V(2) receptor in Madin Darby canine kidney epithelial cells. *Mol Pharmacol*. 2001;60(5):1031-1039.

84. Dong C, Wu G. Regulation of anterograde transport of alpha2-adrenergic receptors by the N termini at multiple intracellular compartments. *J Biol Chem*. 2006;281(50):38543-38554.

85. Juhl C, Kosel D, Beck-Sickinger AG. Two motifs with different function regulate the anterograde transport of the adiponectin receptor 1. *Cell Signal*. 2012;24(9):1762-1769.

86. Rodrigues AR, Sousa D, Almeida H, et al. Cell surface targeting of the Melanocortin 5 Receptor (MC5R) requires serine-rich terminal motifs. *Biochim Biophys Acta*. 2017;1864(7):1217-1226.

87. Gentle IE, Perry AJ, Alcock FH, et al. Conserved motifs reveal details of ancestry and structure in the small TIM

chaperones of the mitochondrial intermembrane space. *Mol Biol Evol*. 2007;24(5):1149-1160.

88. Giraudo CG, Maccioni HJ. Endoplasmic reticulum export of gly-cosyltransferases depends on interaction of a cytoplasmic dibasic motif with Sar1. *Mol Biol Cell*. 2003;14(9):3753-3766.

89. Zaarour N, Demaretz S, Defontaine N, et al. Multiple evolution-arily conserved Di-leucine like motifs in the carboxyl terminus control the anterograde trafficking of NKCC2. *J Biol Chem*. 2012;287(51):42642-42653.

90. Feinstein P, Bozza T, Rodriguez I, Vassalli A, Mombaerts P. Axon guidance of mouse olfactory sensory neurons by odorant receptors and the beta2 adrenergic receptor. *Cell*. 2004;117(6):833-846.

91. Reisert J. Origin of basal activity in mammalian olfactory recep-tor neurons. *J Gen Physiol*. 2010;136(5):529-540.

92. Zhang J, Huang G, Dewan A, Feinstein P, Bozza T. Uncoupling stimulus specificity and glomerular position in the mouse olfac-tory system. *Mol Cell Neurosci*. 2012;51(3–4):79-88.

93. Tsuboi A, Miyazaki T, Imai T, Sakano H. Olfactory sensory neu-rons expressing class I odorant receptors converge their axons on an antero-dorsal domain of the olfactory bulb in the mouse. *Eur J Neurosci*. 2006;23(6):1436-1444.

94. Nakashima AI, Takeuchi H, Imai T, et al. Agonist-independent GPCR activity regulates anterior-posterior targeting of olfactory sensory neurons. *Cell*. 2013;154(6):1314-1325.

95. Stamnes MA, Craighead MW, Hoe MH, et al. An integral mem-brane component of coatomer-coated transport vesicles defines a family of proteins involved in budding. *Proc Natl Acad Sci U S A*. 1995;92(17):8011-8015.

96. Teasdale RD, Jackson MR. Signal-mediated sorting of membrane proteins between the endoplasmic reticulum and the golgi appara-tus. *Annu Rev Cell Dev Biol*. 1996;12:27-54.

97. Park J, Selvam B, Sanematsu K, Shigemura N, Shukla D, Procko E. Structural architecture of a dimeric class C GPCR based on co-trafficking of sweet taste receptor subunits. *J Biol Chem*. 2019;294(13):4759-4774.

98. Zerangue N, Schwappach B, Jan YN, Jan LY. A new ER traffick-ing signal regulates the subunit stoichiometry of plasma mem-brane K(ATP) channels. *Neuron*. 1999;22(3):537-548.

99. Zerangue N, Malan MJ, Fried SR, et al. Analysis of endoplasmic reticulum trafficking signals by combinatorial screening in mam-malian cells. *Proc Natl Acad Sci U S A*. 2001;98(5):2431-2436.

100. Roth D, Lynes E, Riemer J, et al. A di-arginine motif contributes to the ER localization of the type I transmembrane ER oxidore-ductase TMX4. *Biochem J*. 2009;425(1):195-208.

101. Mrowiec T, Schwappach B. 14-3-3 proteins in membrane protein transport. *Biol Chem*. 2006;387(9):1227-1236.

102. Michelsen K, Mrowiec T, Duderstadt KE, et al. A multimeric membrane protein reveals 14-3-3 isoform specificity in forward transport in yeast. *Traffic*. 2006;7(7):903-916.

103. Nufer O, Mitrovic S, Hauri HP. Profile-based data base scan-ning for animal L-type lectins and characterization of VIPL, a novel VIP36-like endoplasmic reticulum protein. *J Biol Chem*. 2003;278(18):15886-15896.

104. Béthune J, Kol M, Hoffmann J, Reckmann I, Brügger B, Wieland F. Coatomer, the coat protein of COPI transport vesicles, discrim-inates endoplasmic reticulum residents from p24 proteins. *Mol Cell Biol*. 2006;26(21):8011-8021.

105. Fiedler K, Veit M, Stamnes MA, Rothman JE. Bimodal interac-tion of coatomer with the p24 family of putative cargo receptors. *Science*. 1996;273(5280):1396-1399.

106. Cosson P, Letourneur F. Coatomer interaction with di-lysine endoplas-mic reticulum retention motifs. *Science*. 1994;263(5153):1629-1631.

107. Gomez M, Scales SJ, Kreis TE, Perez F. Membrane recruitment of coatomer and binding to dilysine signals are separate events. *J Biol Chem*. 2000;275(37):29162-29169.

108. Jackson MR, Nilsson T, Peterson PA. Identification of a consen-sus motif for retention of transmembrane proteins in the endoplas-mic reticulum. *Embo J*. 1990;9(10):3153-3162.

109. Jackson MR, Nilsson T, Peterson PA. Retrieval of transmem-brane proteins to the endoplasmic reticulum. *J Cell Biol*. 1993;121(2):317-333.

110. Nilsson T, Jackson M, Peterson PA. Short cytoplasmic sequences serve as retention signals for transmembrane proteins in the endo-plasmic reticulum. *Cell*. 1989;58(4):707-718.

111. Sester M, Ruszics Z, Mackley E, Burgert HG. The transmembrane domain of the adenovirus E3/19K protein acts as an endoplasmic reticulum retention signal and contributes to intracellular seques-tration of major histocompatibility complex class I molecules. *J Virol*. 2013;87(11):6104-6117.

112. Gidda SK, Shockey JM, Rothstein SJ, Dyer JM, Mullen RT. Arabidopsis thaliana GPAT8 and GPAT9 are localized to the ER and possess distinct ER retrieval signals: functional divergence of the dilysine ER retrieval motif in plant cells. *Plant Physiol Biochem*. 2009;47(10):867-879.

113. Mallouk N, Ildefonse M, Pages F, Ragno M, Bennett N. Basis for intracellular retention of a human mutant of the retinal rod chan-nel alpha subunit. *J Membr Biol*. 2002;185(2):129-136.

114. Rohde HM, Cheong FY, Konrad G, Paiha K, Mayinger P, Boehmelt G. The human phosphatidylinositol phosphatase SAC1 interacts with the coatomer I complex. *J Biol Chem*. 2003;278(52):52689-52699.

115. Mazelova J, Astuto-Gribble L, Inoue H, et al. Ciliary targeting motif VxPx directs assembly of a trafficking module through Arf4. *Embo J*. 2009;28(3):183-192.

116. Jenkins PM, Hurd TW, Zhang L, et al. Ciliary targeting of olfac-tory CNG channels requires the CNGB1b subunit and the kine-sin-2 motor protein, KIF17. *Curr Biol*. 2006;16(12):1211-1216.

117. Dong C, Yang L, Zhang X, et al. Rab8 interacts with distinct motifs in alpha2B- and beta2-adrenergic receptors and differentially mod-ulates their transport. *J Biol Chem*. 2010;285(26):20369-20380.

118. Duvernay MT, Dong C, Zhang X, Zhou F, Nichols CD, Wu G. Anterograde trafficking of G protein-coupled receptors: function of the C-terminal F(X)6LL motif in export from the endoplasmic reticulum. *Mol Pharmacol*. 2009;75(4):751-761.

119. Thielen A, Oueslati M, Hermosilla R, et al. The hydrophobic amino acid residues in the membrane-proximal C tail of the G protein-cou-pled vasopressin V2 receptor are necessary for transport-competent receptor folding. *FEBS Lett*. 2005;579(23):5227-5235.

120. Rivera JF, Ahmad S, Quick MW, Liman ER, Arnold DB. An evo-lutionarily conserved dileucine motif in Shal K+ channels medi-ates dendritic targeting. *Nat Neurosci*. 2003;6(3):243-250.

121. Letourneur F, Klausner RD. A novel di-leucine motif and a tyro-sine-based motif independently mediate lysosomal targeting and endocytosis of CD3 chains. *Cell*. 1992;69(7):1143-1157.

122. Corbit KC, Aanstad P, Singla V, Norman AR, Stainier DY, Reiter JF. Vertebrate Smoothened functions at the primary cilium. *Nature*. 2005;437(7061):1018-1021.

123. Dwyer ND, Adler CE, Crump JG, Noelle DL, Bargmann CI. Polarized dendritic transport and the AP-1 mu1 clathrin adaptor UNC-101 localize odorant receptors to olfactory cilia. *Neuron*. 2001;31(2):277-287.

124. Bermak JC, Li M, Bullock C, et al. Regulation of transport of the dopamine D1 receptor by a new membrane-associated ER protein. *Nat Cell Biol*. 2001;3(5):492-498.

SUPPORTING INFORMATION

Additional Supporting Information may be found online in the Supporting Information section.